LBL-11738 c.2
Preprint

Lawrence Berkeley Laboratory
UNIVERSITY OF CALIFORNIA

Materials & Molecular Research Division

Submitted to Analytical Chemistry

PEAK RESOLUTION BY SEMIDERIVATIVE VOLTAMMETRY

J.J. Toman and S.D. Brown

October 1980

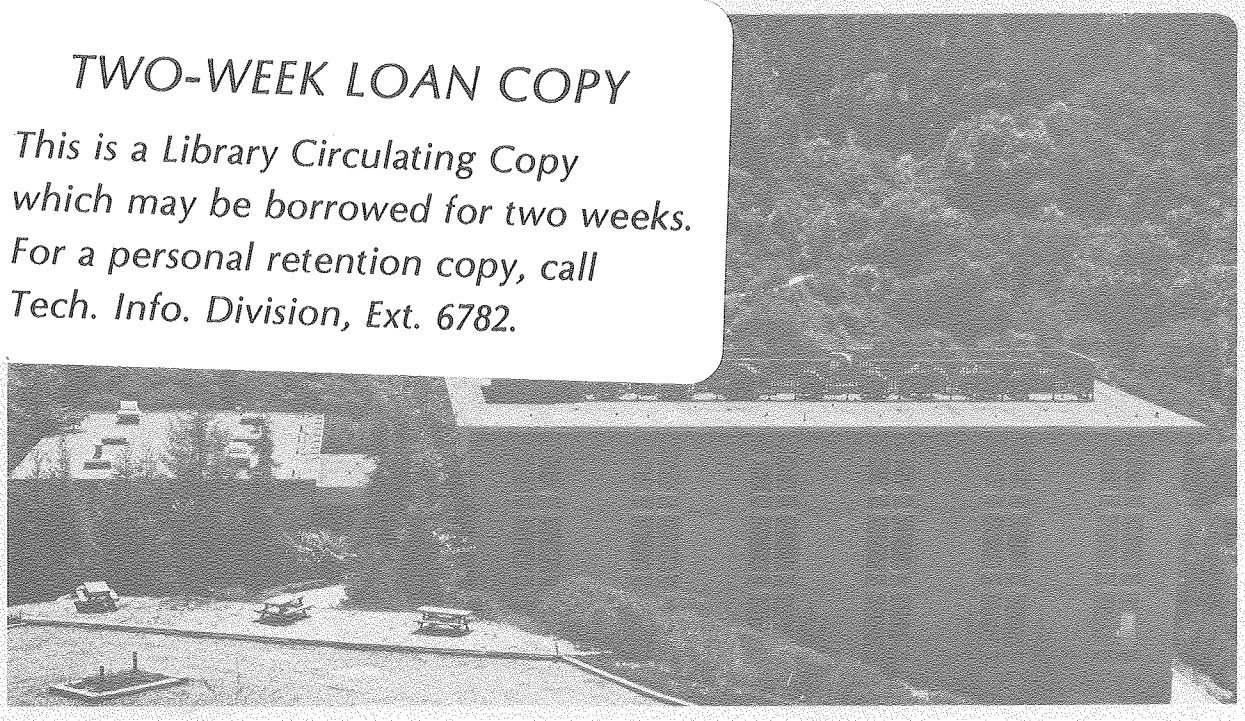

Prepared for the U.S. Department of Energy under Contract W-7405-ENG-48

DISCLAIMER

PEAK RESOLUTION BY SEMIDERIVATIVE VOLTAMMETRY

J. J. Toman and S. D. Brown*

Materials and Molecular Research Division
Lawrence Berkeley Laboratory
and
Department of Chemistry
University of California
Berkeley, CA 94720

October 1980

ABSTRACT

One of the limitations of dynamic electrochemistry, when used as a quantitative analytical technique, is the resolution of overlapping waves. Approaches used in the past have been either time intensive methods using many blanks, or have relied on many empirical peak parameters. Using an approach based on semidifferential voltammetry, two new techniques have been developed for rapid peak deconvolution. The first, NIFIT1, is an iterative stripping routine, while the second, BIMFIT, is based on sequential simplex optimization. Both approaches were characterized by deconvolution of synthetic fused peak systems. Subsequently, both were applied to semidifferentiated linear scan voltammograms of Cd^{2+}, Pb^{2+} and In^{3+}, and to semidifferentiated linear scan anodic stripping voltammograms of Cd^{2+}, In^{3+} and Tl^{+}. Deconvolutions were directly characterized by peak height, peak potential and peak halfwidth, as well as by the total squared deviation of the fit peaks from the real fused peaks. Studies of individual peaks as well as of standard additions to fused peaks showed both

methods worked well, with excellent deconvolution efficiencies. Synthetic data were totally deconvoluted with peak separation as small as 25 mv, while real systems were deconvoluted with separations below 40 mv. Peak parameters obtained from these deconvolutions allow observations of electrode processes, even in systems containing overlapping peaks.

Introduction

A principal difficulty in the use of dynamic electrochemistry as a quantitative analytical technique is the problem of resolution of overlapping waves. This is of particular importance in linear sweep voltammetry (ℓ.s.v.) and anodic stripping voltammetry (a.s.v.) at a stationary mercury electrode because of the very broad, asymmetric nature of the peaks. Another difficulty is that the current-potential relationship is not describable by an analytic function. These problems are particularly unfortunate since ℓ.s.v. instrumentation is easy to use and is relatively inexpensive, and compared to most other dynamic electrochemical techniques offers a wide range of scan rates.

There have been up to now two general approaches to electrochemical peak deconvolution: a "hardware" and a "software" approach. The hardware approach is typified by those of Martin and Shain (1) and Bond and Grabaric (2). In both methods a sample is run along with a blank solution containing a suitable background electrolyte and one of the overlapped components. The concentration of this component is varied until upon subtraction of the blank voltammogram from the sample voltammogram (whether by analog or digital means) no trace of the overlapped component is left. Besides being very time intensive, for cases in which the supporting electrolyte is complex the making of a suitable blank may not even be feasible.

The software approach, that of deconvolution after data taking, is perhaps more promising. Annino (3) divided software deconvolution techniques into two types, time domain and frequency domain. Peak resolution in the frequency domain can be accomplished by the method

of Kirmse and Westerburg (4). In this method the Fourier transform of an overlapped spectrum is divided by the transform of a single component, resulting in a sharpened spectrum. In electrochemistry Binkley and Dessey (5) have recently done work on the least-squares fitting of FT transformed square-wave voltammograms. In this procedure the transform of the overlapped peak is fit with the transforms of single peak data in a least squares manner by varying what would be in the time domain the peak height. This procedure is advantageous in that the fit is reduced in complexity by the reduction of points in going to the frequency domain and in that fits may be done on both real and imaginary parts of the transform in order to obtain an averaged, improved fit. The procedure does rely on utilization of empirical single peak parameters, however.

Time domain deconvolution is curve fitting. Curve fitting of electrochemical data has been hampered by the lack of analytic current-potential functions. Some work has been done in this area, principally by Perone and co-workers (6-8). In their most recent paper (8) of this type Boudreau and Perone describe the application of an empirical peak shape function (the sum of skewed gaussian and cauchy functions) in the use of curve fitting in the deconvolution of square wave voltammetric peaks. This function requires five parameters per peak and in addition requires that three "shape" parameters be found from single peak data. The other two parameters are determined from a least squares minimization procedure. Overlapped peaks with separations as small as 30 mv are determined.

This paper describes a curve fitting peak deconvolution technique for a stationary hanging mercury drop electrode in which ℓ.s.v. or a.s.v. data, after transformation, are fit with a wave shape function that is derived wholly from theory. Reversible ℓ.s.v. voltammograms are transformed via a technique called semidifferential analysis into a form that is exactly equivalent to a $sech^2$ waveform. No empirical single peak parameters are assumed in the curve fitting algorithms, and all fit parameters have a direct physical significance.

Theory

The detailed theory of semiderivative voltammetry has been described elsewhere (9-13). For the application of a linear potential ramp the semiintegral m(E) is defined as (9):

$$m(E) = \pi^{-1/2} \int_{E_i}^{E} \frac{i(\gamma)}{\sqrt{E-\gamma}}\, d\gamma \qquad \text{(Eqn. 1)}$$

and the semiderivative e(E)

$$e(E) = \frac{\partial m(E)}{\partial E} \qquad \text{(Eqn. 2)}$$

For a reversible charge transfer

$$Ox + ne^- = Red \qquad \text{(Eqn. 3)}$$

assuming the appropriate boundary conditions the shape of a semiintegral wave is given by (10):

$$E = E^r_{1/2} + \frac{RT}{nF} \ln\left[\frac{m^* - m(E)}{m(E)}\right] \qquad \text{(Eqn. 4)}$$

where

$$m^* = (D_0 \nu)^{1/2} nFAC^*_{Ox} \qquad \text{(Eqn. 5)}$$

and where D_0 is the diffusion constant of the oxidized species in solution, ν is the scan rate, n is the number of electrons transferred, F is the Faraday constant, A is the surface area of the electrode, and C^*_{Ox} is the bulk concentration of the oxidized species. From application of Eqn. 2 to Eqn. 4 the semiderivative is (12):

$$e(E) = \frac{nFm^*}{4RT} \operatorname{sech}^2\left[\frac{nF}{2RT}(E - E^r_{1/2})\right] \qquad \text{(Eqn. 6)}$$

The semiderivative is seen to be a symmetric peak with a flat baseline. The height of the peak is linearly proportional to the bulk concentration of oxidized species. At 25°C the peak width at half the peak maximum is (12):

$$W_p = \frac{0.0907}{n} V \qquad \text{(Eqn. 7)}$$

For the case of a free metal in equilibrium with N labile metal complexes the semiderivative wave is (9):

$$e(E) = \frac{nFm^*}{4RT} \operatorname{sech}^2 \frac{nF}{2RT}\left\{(E - E^r_{1/2}) + 1/2 \ln \sum_{i=0}^{N} \beta_i [X]^i\right\} \qquad \text{(Eqn. 8)}$$

Formation of labile complexes is seen not to affect the shape of either the semiintegral or semiderivative wave but rather moves them to more negative potentials. The treatment of several electroactive species is also straightforward and results in the linear superposition of semiintegral or semiderivative waves (11).

The above equations for ℓ.s.v. also apply to a.s.v. under certain conditions (9), and in addition the condition that no intermetallic compounds be formed within the mercury drop amalgam. The only difference is that the diffusion constant and bulk concentration of oxidized species are taken as those of the reduced species in the mercury drop. Under certain conditions (14) of short plating time, large volume of solution, and reproducible stirring, metal amalgam concentration is proportional to the bulk oxidized species concentration for equal plating times. Under these conditions both semiderivative and semiintegral waves are proportional to oxidized species bulk concentration.

Experimental

Reagents: For the ℓ.s.v. runs stock solutions of Pb^{2+}, Cd^{2+}, and In^{3+} were made approximately 1.0×10^{-2}M. Metallic A.R. Cd and Pb were dissolved in A.R. HNO_3; it was necessary to dissolve 99.95% In_2O_3 in a minimum amount of hot 72% $HClO_4$. The solutions were titrated with standard EDTA solution and stock solution concentrations of $[Pb^{2+}] = 1.96 \times 10^{-2}$M. $[Cd^{2+}] = 2.09 \times 10^{-2}$M and $[In^{3+}] = 2.02 \times 10^{-2}$M were determined. The supporting electrolyte for these solutions was A.R. HCℓ diluted to 0.58 M.

For the a.s.v. runs Cd^{2+} and In^{3+} stock solutions were diluted to 2.09×10^{-4} M and 2.02×10^{-4}M, respectively, from the stock solutions used in the ℓ.s.v. runs. In addition a $T\ell^{+}$ stock solution was prepared from A.R. TℓNO3, standardized at a concentration of 8.84×10^{-3}M, and an a.s.v. stock solution was diluted to 8.84×10^{-5}M. The a.s.v. supporting electrolyte consisted of purified HCℓ diluted to 0.58 M with water collected from a pre-leached all-vitreous silica still. The HCℓ was purified according to the method of Mattison (15) by sub-boiling distillation. Preleached Teflon® bottles were used to contain the purified HCℓ. All electrochemical cells were carefully cleaned between a.s.v. runs by rinsing with Transistar® grade HNO3.

Cell, Electrodes, and Equipment: The cell and electrodes used in this investigation were the same as those described earlier (9) with the cell thermostatted to 24.9 ± 0.1°C for the l.s.v. experiments and to 23 ± 1°C for the a.s.v. experiments. Equipment used was also described before, with the exception of a solid state relay interfaced with a DAC to control stirring. A Digital Equipment Corporation MINC-11/2B microcomputer was used to control experiments and take data. Another computer with an LSI-11/23 CPU was used for data analysis.

Computer Programs: Control of the ℓ.s.v. and a.s.v. experiments was performed by MACRO-11 assembly language subroutines linked to a FORTRAN driver and other FORTRAN subroutines used for data storage and graphics. Data was stored on disk for later processing. Processing included digital filtering based on fast Fourier transform techniques (16) and semiintegration by a FORTRAN program employing the method of

Huber (17) as given by Nicholson and Olmstead (18). A point by point subtraction program was written to perform a.s.v. background subtraction.

Two different programs were written to deconvolute overlapping peaks. Both fit in a least squares manner experimental semidifferentiated voltammograms with a sum of $sech^2$ functions representing the individual components. The first (NIFIT1) is an iterative stripping routine similar to a method developed for X-ray spectrometry (19). It is completely self starting except for the number of components to be fit in a semidifferentiated voltammogram and the number of iterations to be performed. On the first cycle the maximum of the semidifferentiated voltammogram is found and is used to define the first peak, and then the peak potential and peak height for this peak. A $sech^2$ function is then fit to the side of the peak that is least overlapped by varying the peak width until the sum of the squares of the residuals between calculated and experimental semidifferentiated voltammograms is minimized. The peak made from these three fit parameters is stored in memory and subtracted from the original experimental scan to give a subtracted scan. The process is repeated until calculated peaks for the number of components specified as input are determined.

On the second iteration all but one of the calculated peaks from the first iteration are subtracted from the experimental semidifferentiated voltammogram, resulting in a subtracted semidifferentiated voltammogram of only one peak. The three parameters are then determined from the fit to this peak, and a second order calculated peak is constructed and stored in memory. The process is repeated for the other

peaks until second order peaks have been calculated for all components. The second iteration is then concluded and the program moves to the third iteration. Third order peaks are constructed from second order peaks in the manner just described. The process is concluded when the specified number of iterations have been completed, at which time the final peak potentials, heights, and widths are output.

The second program (BIMFIT) is based on the principle of sequential simplex optimization (20). This program uses the FORTRAN subroutine NELMIN as described by O'Neill (21) based on the algorithm of Nelder and Mead (22). This program takes as input parameters the numeber of peaks, the limiting number of iterations, and the initial guesses of the peak potential, height and width for each peak. The subroutine NELMIN varies all parameters for the fitting function, three for each $sech^2$ peak, simultaneously to minimize the squares of the residuals between experimental semidifferentiated voltammograms and the sum of these $sech^2$ functions with the aid of a user supplied subroutine to calculate the squares of the residuals. The program stops when the specified number of iterations have been completed.

Procedure: For the ℓ.s.v. single peak studies 25 ml. of 0.58 M HCℓ was pipetted into the cell and deaerated with Ar for 5-10 minutes to remove dissolved oxygen. After deaeration, a Hg drop was extruded and a voltammogram taken of the supporting electrolyte from -.200 V to -.900 V vs. the Ag/AgCℓ electrode at a scan rate of 1.0 V/s and written to disk. Then scans were taken of Cd, In, and Pb in different concentrations by adding standard additions of stock solution with an Eppendorf pipette. See Table 1 for a summary

of all solutions studied in this paper.

After all data were taken the voltammograms were digitally filtered, the semiderivative taken and written to disk. Empirically it was found that while the order of filtering and semidifferentiation had no effect on peak potentials, it had a large effect on peak heights. Semiderivative voltammograms obtained by semidifferentiating and then filtering had sloping, non-zero baselines while those made from filtering and then semidifferentiating had flat baselines at nearly zero. The latter case is the result predicted by theory so the order of filtering and then semidifferentiating was used for all voltammograms.

The curve fitting programs NIFIT1 and BIMFIT were then applied to the semiderivative voltammograms with NIFIT1 limited to 10 iterations and BIMFIT limited to 200 iterations. For a semiderivative voltammogram with two peaks, each program required about 15 minutes running time on the LSI-11/23.

The a.s.v. studies were done in the same manner by adding standard additions of freshly made 1.0×10^{-4} M stock solutions to 25 ml of deaerated supporting electrolyte. After deaeration, the potential of the h.m.d.e. was changed to -.235 vs. the Ag/AgCℓ electrode and stirring was instituted to ensure constant flux to the electrode during plating; after 10 seconds the potential was changed to -1.0 V and plating took place for 600 seconds. Six seconds before the end of the plating period stirring was discontinued and the potential changed to -.900 V. This potential was held for 15 seconds to ensure a homogeneous concentration of reduced species within the drop.

Stripping then took place at a scan rate of 1.0 V/s to a final potential of -.200 V.

For each a.s.v. series a scan was first taken of the supporting electrolyte alone to provide a background scan. After all data were taken and digitally filtered the a.s.v. background scans were subtracted point by point from the stripping scans to remove the effects of capacitive current and other background currents (23). The resultant background subtracted voltammograms have the same shape as ℓ.s.v. voltammograms. Subsequently, semidifferentiation and curve fitting techniques were used on these voltammograms exactly as in the ℓ.s.v. runs.

Results and Discussion

The programs NIFIT1 and BIMFIT were characterized by deconvoluting synthetic fused peak systems constructed with the $sech^2$ curve shape. Table 2 gives the results of the fitting for NIFIT1 limited to ten iterations and for BIMFIT limited to 200 iterations. In Table 2 series A, B, and C show respectively the influence of peak potential, peak height, and peak width on the efficiency of the deconvoluting programs. The variable R^2 is the coefficient of determination (24) and is

$$R^2 = 1 - \left\{ \frac{\sum_{i=1}^{N} [Y_i - Y(X_i)]^2}{\sum_{i=1}^{N} Y_i^2} \right\} \qquad \text{(Eqn. 9)}$$

where Y_i is the experimental curve, $Y(X_i)$ is the fit curve, and N= of data points (in all cases=512). Figure 2 shows a synthetic peak and the fit to it along with the deconvoluted components. Results show

that

1) for two peaks of equal height and full width at half maximum (FWHM) of 40 mv (approximately the FWHM for a reversible two-electron charge transfer) deconvolution fails only when ΔE_p, the difference between peak potentials, is less than 20 mv

2) for peaks of 40 mv FWHM and a 10:1 ratio of peak heights NIFIT1 reproduces initial peak parameters better than BIMFIT, BIMFIT failing at about ΔE_p = 30 mv while NIFIT1 begins to fail at about ΔE_p = 20 mv

3) deconvolution efficiency is not reflected solely by 100 R^2 values close to 100. In the B series 100 R^2 values for BIMFIT are all larger than the corresponding NIFIT1 values, yet NIFIT1 much better at reproducing the initial peak parameters

4) for a narrow (40 mv FWHM) peak fused with a broad (60-100 mv FWHM) peak NIFIT1 fails appreciably while BIMFIT does well

5) both programs return initial peak potentials better than either peak heights or widths.

Real systems:

Parameters obtained for fits to real Cd, Pb, and In ℓ.s.v. single peak systems are shown in Table 3. As seen in 3) above, efficiency of deconvolution should not be judged simply on the basis of 100 R^2 values close to 100. Efficiency should be judged on a combination of good 100 R^2 values, precision of deconvoluted peak parameters, and consistency between single peak and multiple peak data. In particular, in agreement with Eqns. 5 and 6 straight line fits of deconvoluted peak height vs. concentration for the added component in each series result in R^2 values close to 1, intercepts near zero, and slopes that remain

nearly constant for each component.

Table 4 lists computed values of average peak potentials and widths for all components of each series, average peak heights for components not added, and the slope, intercept, and R^2 for the straight line fit of concentration to peak height for the added component in each ℓ.s.v. series. In this table and in Table 6, peak parameters for the most dilute component in each series were not included in averages because of the distortion caused by relatively high background noise.

It is seen from Table 3 that NIFIT1 and BIMFIT give nearly identical answers for peak parameters for all systems investigated. Both BIMFIT and NIFIT1 are very good at determining peak potentials in single peak ℓ.s.v. systems, standard deviations for BIMFIT being on the order of 0.5 mv and for NIFIT1 on the order of 1 mv. Peak widths for Cd and Pb are near 45 mv, in good agreement with Eqn. 7 for a reversible charge transfer. The peak width of about 35 mv for the In charge transfer is slightly larger than the predicted 30.2 mv for the reversible case, indicating some degree of non-reversibility and a possible deviation from the $sech^2$ waveform. The 100 R^2 values for the In fits are of the same order as those of the Cd and Pb waveforms, however, indicating that the $sech^2$ waveform remains a good approximation.

The 100 R^2 values in Table 3 and in nearly all of the series increase monotonically with concentration. The increase is due to the lessening relative importance of noise as concentration is increased. Perone (8) has noted the same effect.

Peak height vs. concentration plots for the single peak ℓ.s.v. systems are shown in Figure 3. All three fits have intercepts near the origin,

as in Eqn. 5. The magnitude of the slope agrees qualitatively with the n^2 dependence of Eqn. 5, as the slope of the indium fit is significantly greater than those of the cadmium or lead fits.

Multiple peak ℓ.s.v.: Table 5 shows the data for the ℓ.s.v. multiple peak systems. Average peak parameters and other information are included in Table 4. A representative peak from the SAL series along with the $sech^2$ fit to it and individual components is shown in Figure 4. It is seen that the Pb peak is completely resolved from the In and Cd peaks, which form an overlapped peak system with ΔE_p = 40 mv. Deviations in peak potential are increased over the single peak systems to over one mv, while values of peak potential stay nearly the same as in single peak systems. Peak width values and deviations are nearly the same. Lead peaks show the smallest deviation in peak height, as might be expected for a non-overlapped peak. The indium peaks show the next smallest deviation, while cadmium shows the largest. This is consistent with the supposition that the fit to indium is worse than to the other elements. The fit is to the peak near the peak maximum, while deviation from the $sech^2$ waveform would be expected further away from the maximum, and therefore might not be accounted for in the overlap.

Straight line fits of concentration vs. peak height are shown in Fig. 5. The intercepts, in general, are larger than for the single peak system but are still small. The R^2 values are all close to 1, and the slopes of the individual components all agree well with slopes for the single components. The 100 R^2 values are all close to 100.

Single peak a.s.v.: Table 6 shows the results of studies on single peak a.s.v. systems, and the peak averages and the slopes for the straight

line concentration vs. peak height fits are in Table 7. The plot of the straight line fit for the STL series is in Fig. 6. For the single peak systems peak potential determination is very precise, and the indium potential agrees very well with l.s.v. peak potentials. The peak width of about 90 mv for the Tℓ peak is in good agreement with the 90.7 mv predicted for the theoretical reversible FWHM predicted by Eqn. 5 for a one-electron charge transfer. The peak width of 29 mv for indium is also in agreement with a reversible charge transfer, as opposed to the ℓ.s.v. case. The differing chemical environment of the mercury amalgam as opposed to the bulk solution is responsible for the change. The 100 R^2 values for the fits are of the same order as the ℓ.s.v. fits and show the same increase with concentration. The relatively large intercepts in the intercepts of the straight line fits over the ℓ.s.v. case could be due either to the a.s.v. background subtraction or to the effects of larger background noise. The slope of these two lines again agree qualitatively with results expected from Eqn. 5.

Multiple peak a.s.v.: Data for a.s.v. multiple peak systems are shown in Table 8. As in the ℓ.s.v. multiple peak systems deviations in peak potential are increased over the single peak case, but the average potential is nearly unchanged. Peak width values agree well with single peak data in both value and precision.

The straight line fits of concentration to peak height are shown in Fig. 6. Intercepts are again larger than in the ℓ.s.v. case. The slope of the line in the SCD series matches well with the single peak Tℓ slope. The slopes of the SIN and SALL series are considerably larger, however, though they agree with one another. Fig. 7 shows a peak from

the SIN series and the same peak after the calculated deconvoluted Tℓ peak was subtracted. The remaining peak is of the right shape for a $sech^2$ function for a three electron charge transfer, indicating that the deconvolution process does not account for the increase in peak height. The increase in slope, therefore, does not appear to be due to a flaw in the deconvolution procedure. The increase is possibly due to the formation of intermetallic compounds between thallium and indium in the mercury amalgam. No interaction of these two metals has ever been reported before, but this may be because the overlap of the two peaks makes the system difficult to study. Vydra, et. al. (25) do mention that Tℓ and In both form intermetallic compounds with mercury.

Although any voltammogram may be semidifferentiated, one disadvantage of the model presented in this paper is that the model applies only to the semiderivatives of reversible charge transfers. For reversible systems, though, the application of the $sech^2$ curve fitting procedure to the deconvolution of overlapped ℓ.s.v. and a.s.v. waves is shown to be successful. The procedure results in the direct evaluation of peak parameters useful in thermodynamic, kinetic, and quantitative analyses. In addition it has the advantage of not relying on empirical peak parameters to define the peak shape, so that changes in shape due to charge transfer reversibility or to the occurrence of intermetallic interaction can be noted.

Credit

This work was supported by the U.S. Department of Energy under Contract No. W-7405-ENG-48, and by Contract No. DE AC06-76RL01830-0NWI between Battelle Memorial Institute and the U.S. Department of Energy.

References

1) Martin, K.J.; Shain, I. Anal. Chem. 1958, 30, 1808.

2) Bond, A.M.; Grabaric, B.S. Anal. Chem. 1976, 48, 1624.

3) Annino, R. Adv. Chromatogr. 1977, 15, 33.

4) Kirmse, D.W.; Westerburg, A.W. Anal. Chem. 1971, 43, 1035.

5) Binkley, D.P.; Dessey, R.E. Anal. Chem. 1980, 52, 1335.

6) Perone, S.P.; Gutknecht, W.F. Anal. Chem. 1970, 42, 906.

7) Perone, S.P.; Sybrandt, L.B. Anal. Chem. 1971, 43, 382.

8) Boudreau, P.A.; Perone, S.P. Anal. Chem. 1979, 51, 811.

9) Toman, J.J.; Corn, R.M.; Brown, S.D. Anal. Chim. Acta, in press.

10) Imbeaux, J.C.; Saveant, J.M. J. Electroanal. Chem. 1973, 44, 169.

11) Ammar, F.; Saveant, J.M. J. Electroanal. Chem. 1973, 47, 215.

12) Goto, M.; Ishii, D.J. Electroanal. Chem. 1977, 77, 225.

13) Grenness, M.; Oldham, K.B. Anal. Chem. 1972, 44, 1121.

14) Barendrecht, E. "Stripping Voltammetry" in Electroanal. Chem. vol. 2, A.J. Bard, ed., Dekker: New York, 1967.

15) Mattison, J.M. Anal. Chem. 1972, 44, 1715.

16) Hayes, J.W.; Glover, D.E.; Smith, D.E.; Overton, M.W. Anal. Chem. 1973, 45, 277.

17) Huber, A. Monatsh. Math. Phys. 1939, 47, 240.

18) Nicholson, R.S.; Olmstead, M.C. in Matlson, J.S.; Mark, H.B.; McDonald, H.C. "Electrochemistry", Dekker: New York, 1972.

19) Statham, P.J. Anal. Chem. 1977, 49, 2149.

20) Deming, S.N.; Morgan, S.L. Anal. Chem. 1973, 45(3), 278A.

21) O'Neill, R. Appl. Statistics 1971, 13, 338.

22) Nelder, J.A.; Mead, R. Computer J. 1965, 7, 308.

23) Brown, S.D.; Kowalski, B.R. Anal. Chim. Acta 1979, 107, 13.

24) F. Mosteller and J.W. Tukey "Data Analysis and Regression", Addison Wesley, Reading, Massachusetts, 1977.

25) Vydra, F.; Stulik, K.; Julakova, E. "Electrochemical Stripping Analysis", Wiley and Sons Inc.: New York, 1976.

Table I. Composition of solutions used in this work

L.s.v. systems

All 25 ml of 0.58 M HCl background electrolyte with:

Series

SP: 5-20 µl additions of Pb^{2+} stock solution

SC: 5-20 µl additions of Cd^{2+} stock solution

SI: 5-20 µl additions of In^{3+} stock solution

SIC: 100 µl of In^{3+} stock solution and 5-20 µl additions of Cd^{2+} stock solution

SCI: 100 µl of Cd^{2+} stock solution and 5-20 µl additions of In^{3+} stock solution

SPC: 100 µl of Pb^{2+} stock solution and 5-20 µl additions of Cd^{2+} stock solution

SAL: 100 µl of both Pb^{2+} and In^{3+} stock solution and 5-20 µl additions of Cd^{2+} stock solution

L.s.v. stock solution concentrations:

$[Pb^{2+}] = 1.96 \times 10^{-2}$ M $\quad [Cd^{2+}] = 2.09 \times 10^{-2}$ M $\quad [In^{3+}] = 2.02 \times 10^{-2}$ M

A.s.v. systems

All 25 ml of 0.58 M purified HCℓ background electrolyte with:

Series

STL: 5-20 µl additions of $Tℓ^{+}$ stock solution

SINA: 6-20 µl additions of In^{3+} stock solution

SCD: 50 µl of Cd^{2+} stock solution and 5-20 µl additions of $Tℓ^{+}$ stock solution

SIN: 20 µl of In^{3+} stock solution and 5-20 µl additions of $Tℓ^{+}$ stock solution

SALL: 20 µl of both Cd^{2+} and In^{3+} stock solution and 5-20 µl additions of $Tℓ^{+}$ stock solution

A.s.v. stock solution concentrations:

$[Tℓ^{+}] = 8.84 \times 10^{-5}$ M $\quad [In^{3+}] = 2.02 \times 10^{-4}$ M $\quad [Cd^{2+}] = 2.09 \times 10^{-4}$ M

Table II. Fit peak aparameters for synthetic $sech^2$ fused peak systems using programs BIMFIT and NIFIT1[a]

Series	Potl.[b]	Height[b]	Width[b]	Potl.[b]	Height[b]	Width[b]	100 R^2
AA	-.35	1.0	40.0	-.5	1.0	40.0	
	-.3500	1.0026	40.36	-.5002	1.0001	39.87	99.99
	-.3502	0.9998	40.06	-.4499	0.9988	40.06	99.99
AB	-.4	1.0	40.0	-.5	1.0	40.0	
	-.3999	0.9999	40.01	-.4999	0.9994	40.00	99.99
	-.3996	0.9981	40.06	-.4999	0.9980	40.06	99.99
AC	-.42	1.0	40.0	-.5	1.0	40.0	
	-.4199	1.0012	39.91	.4999	0.9993	40.05	99.99
	-.4204	0.9989	40.06	-.4999	0.9987	40.06	99.99
AD	-.435	1.0	40.0	-.5	1.0	40.0	
	-.4349	0.9999	40.01	-.4999	1.0000	39.99	99.99
	-.4343	0.9994	39.88	-.4999	0.9994	40.06	99.97
AE	-.45	1.0	40.0	-.5	1.0	40.0	
	-.4500	0.9997	40.35	-.4999	0.9960	39.92	99.99
	-.4500	0.9983	38.32	-.4994	1.0068	40.06	99.96
AF	-.46	1.0	40.0	-.5	1.0	40.0	
	-.4597	0.9928	39.93	-.4995	1.0099	39.96	99.99
	-.4598	0.9890	36.72	-.4989	1.0302	41.38	99.93
AG	-.47	1.0	40.0	-.5	1.0	40.0	
	-.4686	0.9590	38.59	-.4988	1.0592	40.38	99.99
	-.4676	0.8529	31.48	-.4970	1.1743	41.97	99.72
AH	-.48	1.0	40.0	-.5	1.0	40.0	
	-.4690	0.2352	25.63	-.4919	1.6459	45.34	99.96
	-.4891	1.6303	48.97	-.5048	0.1119	20.26	99.89

a) The first line for each series gives actual input peak parameters. The next two lines give the output parameters for BIMFIT and NIFIT1.

b) Units for potentials are in volts; those for widths in mv; current units are arbitrary.

Table II. (continued)

Series	Potl.[b]	Height[b]	Width[b]	Potl.[b]	Height[b]	Width[b]	100 R^2
BA	-.45	0.1	40.0	-.5	1.0	40.0	
	-.4496	0.0995	39.76	-.4999	0.9999	40.15	99.99
	-.4498	0.0984	40.06	-.4999	0.9990	40.06	99.99
BB	-.46	0.1	40.0	-.5	1.0	40.0	
	-.4593	0.0981	39.64	-.4998	1.0025	40.09	99.99
	-.4603	0.0999	44.07	-.4999	0.9942	40.06	99.99
BC	-.47	0.1	40.0	-.5	1.0	40.0	
	-.4762	0.1378	46.21	-.5005	0.9576	39.31	99.99
	-.4715	0.1008	44.07	-.5004	0.9895	40.06	99.98
BD	-.475	0.1	40.0	-.5	1.0	40.0	
	-.4870	0.2405	46.51	-.5012	0.8436	38.91	99.99
	-.4754	0.1032	44.07	-.4999	0.9900	40.06	99.99
BE	-.48	0.1	40.0	-.5	1.0	40.0	
	-.4882	0.3470	40.13	-.5026	0.7911	37.80	99.99
	-.4754	0.0769	44.07	-.4992	1.0155	40.06	99.95

Table II. (continued)

Series	Potl.[b]	Height[b]	Width[b]	Potl.[b]	Height[b]	Width[b]	100 R^2
CA	-.45	1.0	10.0	-.5	1.0	40.0	99.99
	-.4500	0.9961	10.08	-.5000	0.9993	39.70	99.97
	-.4500	0.9994	10.49	-.4999	0.9988	40.06	
CB	-.45	1.0	20.0	-.5	1.0	40.0	
	-.4500	1.0013	19.77	-.4998	1.0024	40.06	99.99
	-.4500	1.0035	20.50	-.4999	0.9978	39.31	99.98
CC	-.45	1.0	30.0	-.5	1.0	40.0	
	-.4500	1.0001	30.00	-.5000	1.0000	39.98	99.99
	-.4500	0.9997	30.39	-.4999	0.9978	40.06	99.99
CD	-.45	1.0	50.0	-.5	1.0	40.0	
	-.4500	1.0001	49.97	-.5000	1.0003	40.00	99.99
	-.4500	0.9962	47.44	-.4994	1.0170	41.57	99.95
CE	-.45	1.0	60.0	-.5	1.0	40.0	
	-.4500	1.0002	59.99	-.5000	1.0003	39.99	99.99
	-.4495	0.9829	55.09	-.4992	1.0481	40.06	99.87
CF	-.45	1.0	80.0	-.5	1.0	40.0	
	-.4499	0.9994	79.89	-.5000	1.0027	40.05	99.99
	-.4480	0.9614	63.41	-.4989	1.1688	44.07	99.42
CG	-.45	1.0	90.0	-.5	1.0	40.0	
	-.4499	1.0028	89.29	-.5001	0.9985	40.29	99.99
	-.4461	0.9517	67.80	-.4989	1.2282	44.83	99.29
CH	-.45	1.0	100.0	-.5	1.0	40.0	
	-.4495	0.9941	99.44	-.5000	1.0075	40.77	99.99
	-.4441	0.9367	69.45	-.4989	1.3046	46.72	98.92

Table III. Fit peak parameters for l.s.v. single peak data using programs BIMFIT and NIFITl

Series	Pb				Cd				
	Conc.[b]	Potl.[b]	Height[b]	Width[b]	Conc.[b]	Potl.[b]	Height[b]	Width[b]	100 R^2
SP1[a]	1.57	-.4784	0.577	50.7					80.70
		-.4791	0.589	47.6					80.43
SP2	3.14	-.4783	1.105	47.8					94.87
		-.4774	1.135	46.4					94.82
SP3	4.72	-.4777	1.616	46.3					97.19
		-.4780	1.619	45.2					97.18
SP4	6.29	-.4781	2.189	44.6					98.60
		-.4789	2.209	42.8					98.33
SP5	7.86	-.4778	2.684	46.1					99.00
		-.4779	2.691	44.1					98.70
SP6	9.42	-.4776	3.175	45.0					99.25
		-.4775	3.168	43.4					99.06
SC1					1.67	-.6875	0.426	34.3	64.64
						-.6871	0.411	44.1	61.77
SC2					3.34	-.6875	0.843	41.4	91.52
						-.6883	0.812	44.1	91.36
SC3					5.01	-.6878	1.354	41.5	97.18
						-.6877	1.342	44.1	96.99
SC4					6.68	-.6871	1.900	42.5	98.64
						-.6867	1.859	44.1	98.53
SC5					8.36	-.6872	2.281	44.3	99.11
						-.6879	2.252	44.1	99.10

a) The top line of each series gives the BIMFIT results, the bottom the NIFITl results
b) Units for concentration are 1.0×10^{-5} M , for potential are V vs. the Ag/AgCℓ electrode, for peak height are μA/s(1/2), and for width are mv.

Table III (continued)

Series	In				
	Conc.[b]	Potl.[b]	Height[b]	Width[b]	100 R^2
SI1	1.62	-.6513	0.650	32.0	86.60
		-.6492	0.627	36.7	84.89
SI2	3.24	-.6516	1.342	33.4	95.79
		-.6503	1.313	32.6	95.11
SI3	4.85	-.6510	1.900	35.2	98.07
		-.6503	1.878	35.3	97.85
SI4	6.47	-.6511	2.610	36.1	98.76
		-.6503	2.591	35.3	98.48
SI5	8.09	-.6506	3.352	35.9	99.13
		-.6493	3.313	33.4	98.25

Table IVa: Average peak parameters and results of straight line fits of concentration to peak height for l.s.v. data using BIMFIT

	Cd			In			Pb					
Series	Potl.[c]	Height[c]	Width[c]	Potl.	Height	Width	Potl.	Height	Width	Slope[a,b]	Intercept[a,b]	R^{2}[a]
SC	-.6874± 0.0003		42.4± 1.3							0.285	-0.068	0.9968
SP							-.4779± 0.0003		45.9± 1.2	0.333	0.060	0.9996
SI				-.6511± 0.0004		35.2± 1.2				0.413	-0.032	0.9979
SIC	-.6903± 0.0011		45.7± 1.2	-.6530± 0.0011	2.426± 0.054	33.4± 0.9				0.286	0.115	0.9978
SCI	-.6915± 0.0012	2.496± 0.122	44.8± 1.4	-.6520± 0.0012		33.1± 0.8				0.389	0.170	0.9987
SPC	-.6896± 0.0005		42.6± 1.6				-.4819± 0.0023	2.584± 0.054	45.6± 0.6	0.297	-0.098	0.9959
SAL	-.6886± 0.0028		45.0± 1.2	-.6499± 0.0018	3.317± 0.088	34.5± 0.7	-.4799± 0.0014	2.697± 0.055	45.7± 1.1	0.279	0.263	0.9954

a) Slope, intercept and R^{2} refer to the least-squares straight line fit of the concentration of added species in each series to peak height.
b) Units for slope and intercept are μA/[s(1/2)·1.0E-05 M] and μA/s(1/2), respectively.
c) Units for potential are V vs. Ag/AgCℓ electrode, for height are μA/s(1/2) for width are mv.

Table IVb: Average peak parameters and results of straight line fits of concentration to peak height for l.s.v. data using NIFITI

	Cd			In			Pb					
Series	Potl.	Height	Width	Potl.	Height	Width	Potl.	Height	Width	Slope	Intercept	R^2
SC	-.6876± 0.0007		44.1							0.282	-0.082	0.9970
SP							-.4779± 0.0006		44.4± 1.4	0.330	0.086	0.9991
SI				-.6500± 0.0005		34.2± 1.3				0.411	-0.052	0.9984
SIC	-.6901± 0.0015		46.7± 2.4	-.6526± 0.0010	2.336± 0.102	33.1± 0.8				0.275	0.158	0.9934
SCI	-.6915± 0.0013	2.467± 0.107	45.1± 1.6	-.6518± 0.0016		33.3± 1.5				0.390	0.105	0.9970
SPC	-.6896± 0.0005		42.6± 1.6				-.4819± 0.0023	2.584± 0.054	45.6± 0.6	0.298	-0.126	0.9955
SAL	-.6880± 0.0030		46.3± 1.9	-.6499± 0.0018	3.317± 0.088	34.5± 0.7	-.4802± 0.0015	2.704± 0.057	44.9± 1.0	0.273	0.310	0.9963

Table Va: Fit peak parameters for l.s.v. multiple peak data using BIMFIT[a]

Series	Cd				In				Pb				
	Conc.	Potl.	Height	Width	Conc.	Potl.	Height	Width	Conc.	Potl.	Height	Width	100 R^2
SIC1					8.09	-.6550	2.465	35.0					98.29
SIC120	1.67	-.6868	0.616	44.1	8.09	-.6535	2.432	32.8					98.65
SIC140	3.34	-.6891	1.023	46.9	8.09	-.6529	2.390	33.2					98.87
SIC160	5.01	-.6917	1.585	44.2	8.09	-.6530	2.508	33.8					99.27
SIC180	6.69	-.6901	2.001	45.5	8.09	-.6522	2.394	33.0					99.39
SIC100	8.36	-.6902	2.519	46.2	8.09	-.6517	2.365	32.5					99.53
SCI1	8.36	-.6920	2.301	43.2									98.93
SCI120	8.36	-.6928	2.433	43.0	1.62	-.6548	0.814	33.5					99.31
SCI140	8.36	-.6911	2.470	44.7	3.24	-.6520	1.453	32.3					99.36
SCI160	8.36	-.6905	2.534	45.7	4.85	-.6514	1.999	33.3					99.46
SCI180	8.36	-.6897	2.614	46.4	6.47	-.6509	2.676	32.7					99.58
SCI100	8.36	-.6927	2.622	45.5	8.09	-.6537	3.347	34.1					99.58
SPC1									7.86	-.4852	2.679	44.7	99.06
SPC120	1.67	-.6934	0.377	37.6					7.86	-.4845	2.534	44.9	99.43
SPC140	3.34	-.6904	0.884	40.6					7.86	-.4808	2.563	46.1	99.49
SPC160	5.01	-.6895	1.477	41.9					7.86	-.4804	2.605	45.9	99.52
SPC180	6.69	-.6892	1.842	43.6					7.86	-.4801	2.582	45.8	99.55
SPC100	8.36	-.6894	2.385	44.1					7.86	-.4803	2.538	46.0	99.69
SAL11					8.09	-.6504	3.454	35.7	7.86	-.4797	2.793	45.3	99.39
SAL120	1.67	-.6847	0.709	43.6	8.09	-.6489	3.306	34.0	7.86	-.4797	2.672	46.8	99.56
SAL140	3.34	-.6873	1.162	46.2	8.09	-.6492	3.315	34.4	7.86	-.4794	2.726	45.5	99.57
SAL160	5.01	-.6875	1.739	45.0	8.09	-.6489	3.290	34.1	7.86	-.4791	2.654	47.2	99.64
SAL180	6.69	-.6867	2.150	45.2	8.09	-.6485	3.183	33.7	7.86	-.4790	2.644	44.0	99.66
SAL100	8.36	-.6928	2.549	43.4	8.09	-.6532	3.354	34.9	7.86	-.4827	2.690	45.6	99.76

a) For units of parameters see Table III.

Table Vb: Fit peak parameters for l.s.v. multiple peak data using NIFIT1

Series	Cd				In				Pb				
	Conc.	Potl.	Height	Width	Conc.	Potl.	Height	Width	Conc.	Potl.	Height	Width	100 R^2
SIC1					8.09	-.6543	2.439	33.8					97.94
SIC120	1.67	-.6734	0.678	39.0	8.09	-.6522	2.181	31.9					97.51
SIC140	3.34	-.6885	0.991	50.1	8.09	-.6529	2.296	33.4					98.84
SIC160	5.01	-.6922	1.559	44.7	8.09	-.6529	2.456	34.2					99.24
SIC180	6.69	-.6898	1.961	45.4	8.09	-.6517	2.347	32.8					99.27
SIC100	8.36	-.6900	2.492	46.6	8.09	-.6515	2.299	32.6					99.50
SCI1	8.36	-.6913	2.285	42.8									98.73
SCI120	8.36	-.6925	2.417	43.8	1.62	-.6541	0.765	32.8					99.31
SCI140	8.36	-.6911	2.462	45.7	3.24	-.6514	1.394	31.6					99.37
SCI160	8.36	-.6908	2.500	46.4	4.85	-.6514	1.921	33.9					99.46
SCI180	8.36	-.6897	2.569	47.1	6.47	-.6504	2.596	32.6					99.50
SCI100	8.36	-.6935	2.569	45.0	8.09	-.6541	3.319	35.1					99.59
SPC1									7.86	-.4858	2.679	43.2	99.03
SPC120	1.67	-.6925	0.339	41.2					7.86	-.4846	2.526	44.3	99.40
SPC140	3.34	-.6914	0.867	39.4					7.86	-.4817	2.588	43.8	99.42
SPC160	5.01	-.6890	1.453	41.6					7.86	-.4806	2.609	46.1	99.50
SPC180	6.69	-.6897	1.817	44.1					7.86	-.4803	2.577	45.0	99.57
SPC100	8.36	-.6897	2.543	44.5					7.86	-.4804	2.540	45.0	99.70
SAL11					8.09	-.6490	3.424	33.0	7.86	-.4799	2.796	45.2	98.79
SAL120	1.67	-.6843	0.747	45.2	8.09	-.6486	3.236	33.5	7.86	-.4802	2.707	44.5	99.54
SAL140	3.34	-.6856	1.195	49.0	8.09	-.6486	3.186	33.8	7.86	-.4802	2.735	43.8	99.52
SAL160	5.01	-.6869	1.751	46.4	8.09	-.6486	3.192	33.8	7.86	-.4789	2.634	46.6	99.62
SAL180	6.69	-.6869	2.138	45.4	8.09	-.6486	3.133	33.8	7.86	-.4789	2.665	45.0	99.69
SAL100	8.36	-.6924	.2556	44.5	8.09	-.6527	3.253	34.3	7.86	-.4830	2.689	44.3	99.73

Table VI: Fit peak parameters for a.s.v. single peak data using programs BIMFIT AND NIFIT1[a]

	Tl				In				
Series	Conc.	Potl.	Height	Width	Conc.	Potl.	Height	Width	100 R^2
STL1[b]	0.707	-.5429	0.0745	96.9					86.13
STL2	1.41	-.5436	0.1273	92.8					95.10
		-.5461	0.1287	84.8					97.69
STL3	2.12	-.5435	0.1718	93.3					98.00
		-.5436	0.1749	87.3					97.73
STL4	2.83	-.5434	0.2227	91.7					99.25
		-.5425	0.2225	88.1					99.11
STL5	3.54	-.5437	0.2769	95.0					98.91
		-.5414	0.2805	84.8					98.05
SINA1					1.62	-.6489	0.541	27.5	85.97
						-.6478	0.542	24.0	84.09
SINA2					3.24	-.6491	1.271	29.8	97.44
						-.6482	1.257	28.2	96.39
SINA3					4.85	-.6493	2.028	28.8	98.10
						-.6492	1.987	28.6	97.97
SINA4					6.47	-.6490	2.646	29.1	98.73
						-.6482	2.608	27.8	97.79
SINA5					8.09	-.6489	3.484	28.8	99.07
						-.6482	3.412	27.8	98.25
SINA6					9.70	-.6489	4.233	28.9	99.13
						-.6482	4.150	28.1	98.36

[a]Concentration units are 1.0E-07 M. For other units and table format see Table III.

[b]NIFIT1 deconvolution unsuccessful due to low signal.

Table VIIa: Average peak parameters and results of straight line fits of concentration to peak height for a.s.v. data using BIMFIT[a]

	Cd			In			Tℓ					
Series	Potl.	Height	Width	Potl.	Height	Width	Potl.	Height	Width	Slope	Intercept	R^2
STL							-.5436± 0.0001		93.1± 1.5	0.0706	0.0249	0.9890
SINA				-.6490± 0.0002		29.1± 0.4				0.4546	-0.2065	0.9990
SCD	-.6936± 0.0002	1.1300± 0.0167	46.5± 0.3				-.5445± 0.0023		100.0± 1.7	0.0723	0.0310	0.9953
SIN				-.6511± 0.0006	0.7292± 0.0406	28.4± 0.2	-.5415± 0.0008		92.8± 0.9	0.0925	-0.0036	0.9975
SALL	-.6924± 0.0006	0.6139± 0.0104	48.0± 1.2	-.6497± 0.0005	0.8008± 0.0232	27.5± 1.1	-.5418± 0.0026		88.7± 6.2	0.0980	0.0395	0.9962

[a]All concentration units are 1.0E-0.7 M, otherwise see Table IVa for explanation of table format and other units.

Table VIIb: Average peak parameters and results of straight line fits of concentration to peak height for a.s.v. data using NIFITI

Series	Cd Potl.	Cd Height	Cd Width	In Potl.	In Height	In Width	Tℓ Potl.	Tℓ Height	Tℓ Width	Slope	Intercept	R^2
STL							-.5434± 0.0020		86.2± 1.7	0.0708	0.0263	0.9969
SINA				0.6484± 0.0004		28.1± 0.3				0.4442	-0.1887	0.9992
SCD	-.6936± 0.0004	1.1322± 0.0168	46.1± 0.2				-.5434± 0.0012		98.5± 2.3	0.0747	0.0243	0.9970
SIN				-.6507± 0.0006	0.7149± 0.0408	28.4± 0.2	-.5440± 0.0017		84.9± 6.2	0.0910	0.0035	0.9988
SALL	-.6932± 0.0005	0.6130± 0.0066	42.5± 0.2	-.6505± 0.0006	0.8006± 0.0108	29.9± 0.3	-.5450± 0.0015		90.4± 1.2	0.1027	0.0200	0.9995

Table VIIIa: Fit peak parameters for a.s.v. multiple peak data using BIMFIT

	Cd				In				Tℓ				
Series	Conc.[a]	Potl.	Height	Width	Conc.[a]	Potl.	Height	Width	Conc.[a]	Potl.	Height	Width	100 R^2
SCD1	4.18	-.6935	1.136	46.6									99.75
SCD2	4.18	-.6933	1.148	46.9					0.707	-.5358	0.0876	94.5	99.80
SCD3	4.18	-.6936	1.114	46.0					1.41	-.5474	0.1241	97.5	99.69
SCD4	4.18	-.6936	1.149	46.3					2.12	-.5419	0.1875	101.3	99.85
SCD5	4.18	-.6938	1.122	46.3					2.83	-.5446	0.2343	100.2	99.88
SCD6	4.18	-.6936	1.111	46.7					3.54	-.5440	0.2885	100.9	99.92
SIN1					1.62	-.6521	0.6722	28.4					98.34
SIN2					1.62	-.6514	0.6950	28.3	0.707	-.5381	0.0668	98.5	99.17
SIN3					1.62	-.6510	0.7272	28.2	1.41	-.5404	0.1244	93.9	99.16
SIN4					1.62	-.6509	0.7386	28.8	2.12	-.5419	0.1884	92.8	99.45
SIN5					1.62	-.6507	0.7600	28.3	2.83	-.5415	0.2533	92.6	99.76
SIN6					1.62	-.6506	0.7819	28.5	3.54	-.5421	0.3300	91.7	99.53
SALL1	1.67	-.6912	0.6115	47.9	1.62	-.6490	0.8230	25.7					99.67
SALL2	1.67	-.6928	0.6341	46.0	1.62	-.6498	0.8219	28.0	0.707	-.5416	0.1103	67.6	99.81
SALL3	1.67	-.6925	0.6084	47.6	1.62	-.6498	0.8040	28.6	1.41	-.5392	0.1835	80.8	99.79
SALL4	1.67	-.6928	0.6148	49.0	1.62	-.6505	0.7936	26.9	2.12	-.5448	0.2364	95.1	99.75
SALL5	1.67	-.6924	0.6060	49.3	1.62	-.6495	0.7598	27.6	2.83	-.5401	0.3154	91.6	99.75
SALL6	1.67	-.6924	0.6084	48.4	1.62	-.6498	0.8027	28.3	3.54	-.5431	0.3916	87.1	99.86

a) Concentration units are 1.0E-07 M; all other units are as in Table Va.

Table VIIIb: Fit peak parameters for a.s.v. multiple peak data using NIFIT1

	Cd				In				Tℓ				
Series	Conc.	Potl.	Height	Width	Conc.	Potl.	Height	Width	Conc.	Potl.	Height	Width	100 R^2
SCD1	4.18	-.6935	1.1394	46.4									99.75
SCD2	4.18	-.6932	1.1517	46.4					0.707	-.5374	0.0803	90.9	99.78
SCD3	4.18	-.6935	1.1121	46.2					1.41	-.5421	0.1228	101.3	99.69
SCD4	4.18	-.6932	1.1493	45.9					2.12	-.5449	0.1872	95.8	99.81
SCD5	4.18	-.6940	1.1202	45.9					2.83	-.5428	0.2334	97.9	99.84
SCD6	4.18	-.6940	1.1204	45.9					3.54	-.5437	0.2895	99.0	99.92
SIN1					1.62	-.6517	0.6569	28.2					98.17
SIN2					1.62	-.6510	0.6785	28.5	0.707	-.5434	0.0713	78.7	98.94
SIN3					1.62	-.6505	0.7125	28.5	1.41	-.5461	0.1291	76.0	98.82
SIN4					1.62	-.6503	0.7310	28.2	2.12	-.5421	0.1956	89.0	99.25
SIN5					1.62	-.6503	0.7479	28.3	2.83	-.5442	0.2574	85.6	99.54
SIN6					1.62	-.6503	0.7628	28.6	3.54	-.5436	0.3296	89.0	99.42
SALL1	1.67	-.6928	0.6100	42.4	1.62	-.6503	0.7975	29.7					99.75
SALL2	1.67	-.6932	0.6230	42.6	1.62	-.6503	0.8133	29.8	0.707	-.5491	0.0902	73.4	99.74
SALL3	1.67	-.6928	0.6164	42.8	1.62	-.6503	0.8002	29.6	1.41	-.5449	0.1655	91.8	99.74
SALL4	1.67	-.6942	0.6090	42.4	1.62	-.6517	0.8052	29.8	2.12	-.5463	0.2414	90.9	99.69
SALL5	1.67	-.6928	0.6043	42.6	1.62	-.6503	0.7814	30.0	2.83	-.5458	0.3109	89.0	99.63
SALL6	1.67	-.6932	0.6152	42.4	1.62	-.6503	0.8058	30.3	3.54	-.5428	0.3815	89.9	99.78

Figure Captions

Figure 1. Fourier transform filtered ℓ.s.v. scan of lead at 9.42 x10^{-5} M with the corresponding semiderivative.

Figure 2. Synthetic fused peak AE with resolved components (See Table 2).

Figure 3. Peak height vs. concentration plots with corresponding fit straight lines for the single peak ℓ.s.v. systems.

Key to symbols: □ = SP series
△ = SC series
+ = SI series

Figure 4. Real semidifferentiated peak with corresponding BIMFIT fit.

Figure 5. Peak height vs. concentration plots with corresponding straight lines for the multiple peak ℓ.s.v. systems.

Key to symbols: □ = SIC series
⬡ = SCI series
△ = SPC series
+ = SALL series

Figure 6. Peak height vs. concentration plots with corresponding straight line fits for the $T\ell^+$ a.s.v. single peak and a.s.v. multiple peaks systems.

Key to symbols: □ = STL series
⬡ = SCD series
△ = SIN series
+ = SALL series

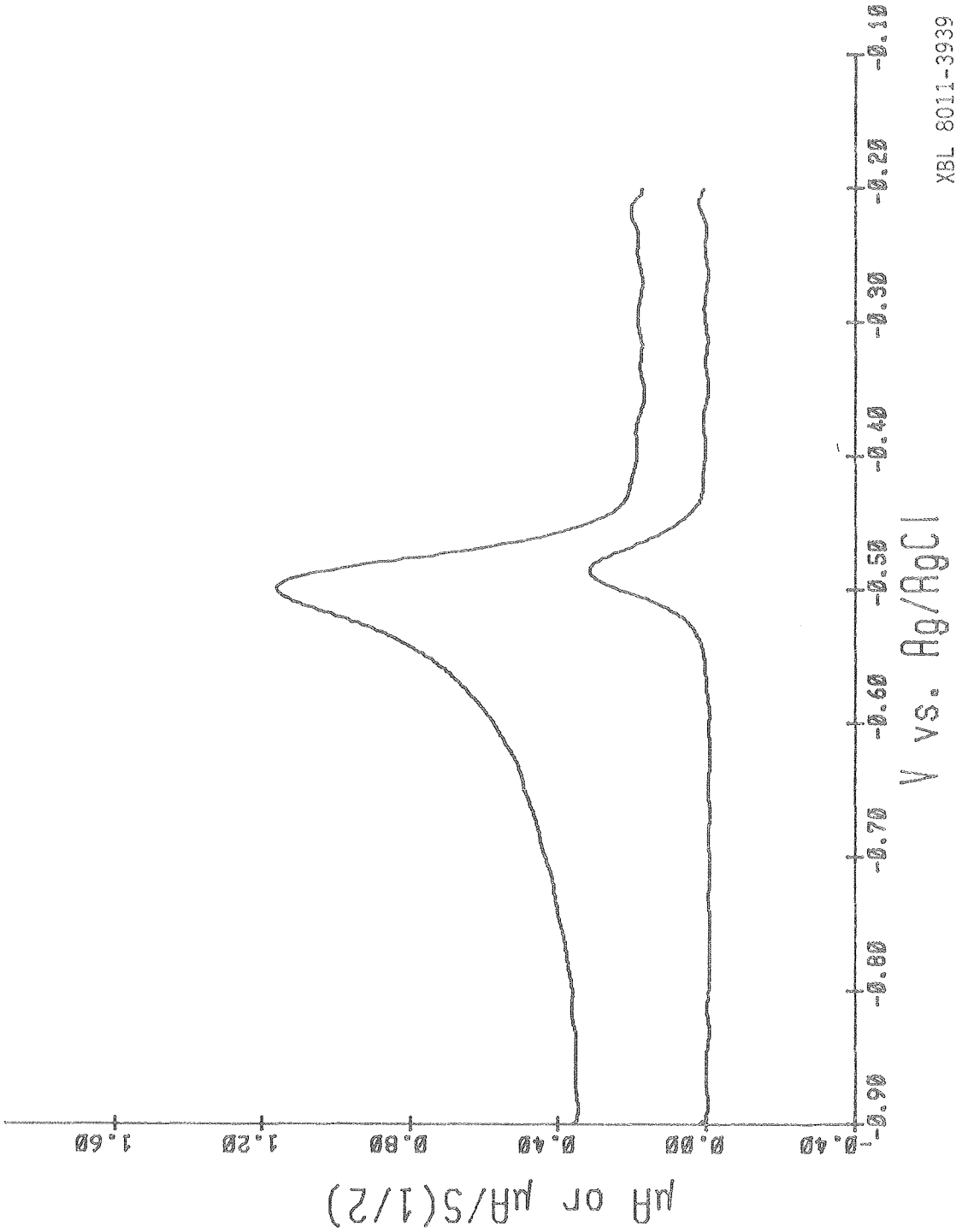
μA or μA/S(1/2)
1.60
1.20
0.80
0.40
0.00
-0.40
-0.90
-0.80
-0.70
-0.60
-0.50
-0.40
-0.30
-0.25
-0.10
V vs. Ag/AgCl
XBL 8011-3939

Figure 1

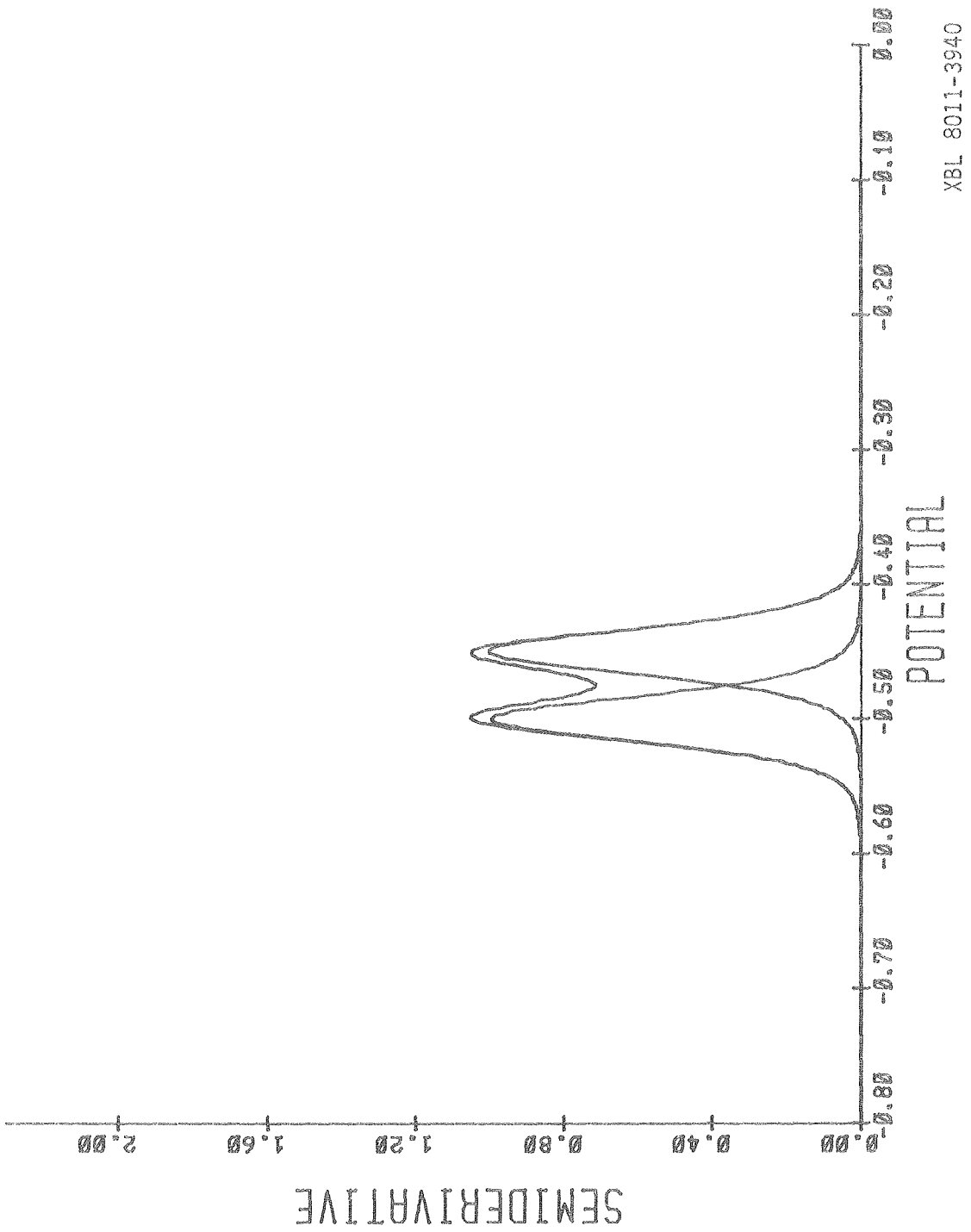
SEMIDERIVATIVE
0.00
0.40
0.80
1.20
1.60
2.00
-0.80
-0.70
-0.60
-0.50
-0.40
-0.30
-0.20
-0.10
0.00
POTENTIAL
XBL 8011-3940

Figure 2

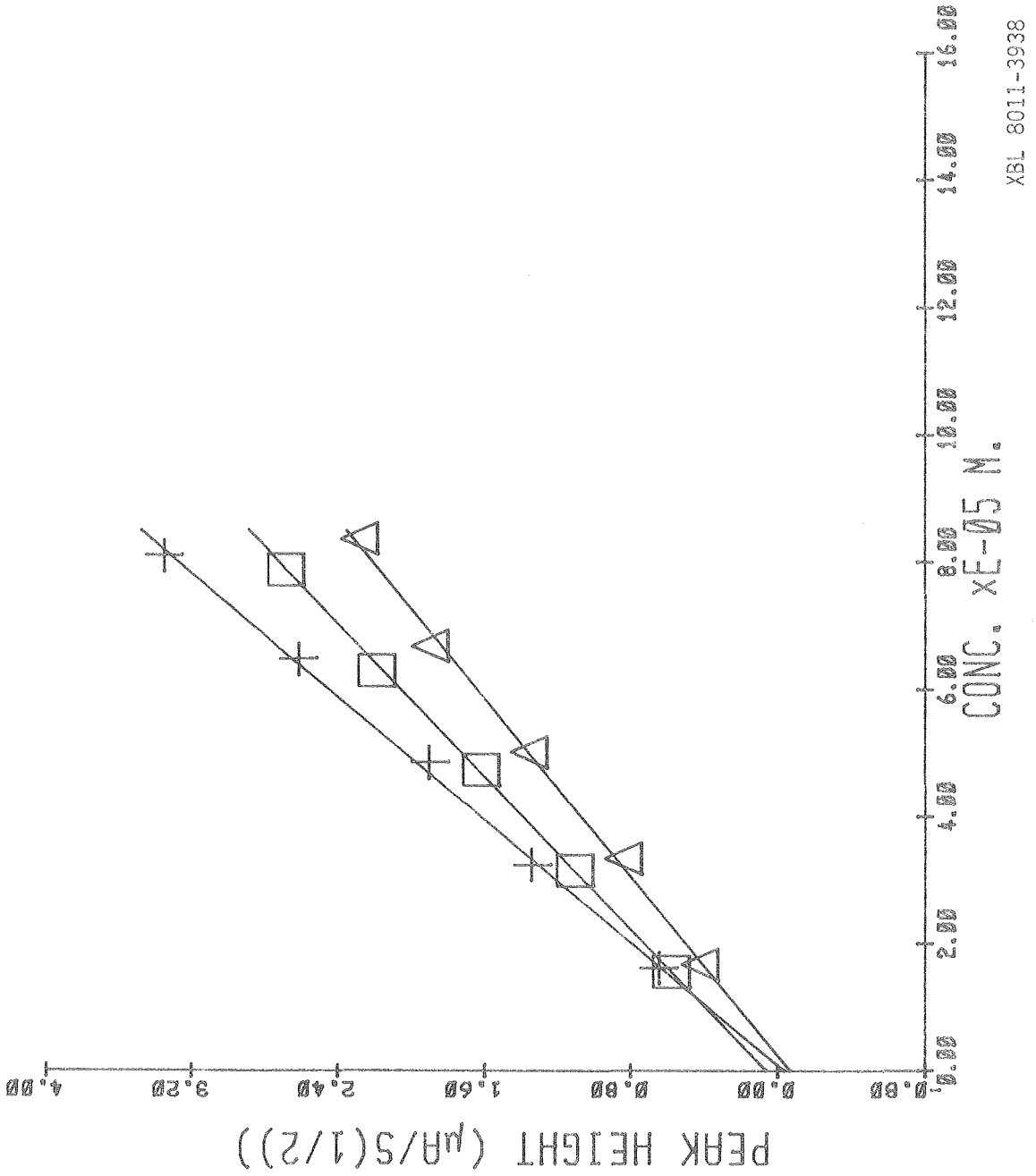
PEAK HEIGHT (μA/S(1/2))
0.00
0.80
1.60
2.40
3.20
4.00
0.00
2.00
4.00
6.00
8.00
10.00
12.00
14.00
16.00
CONC. xE-05 M.
XBL 8011-3938

Figure 3

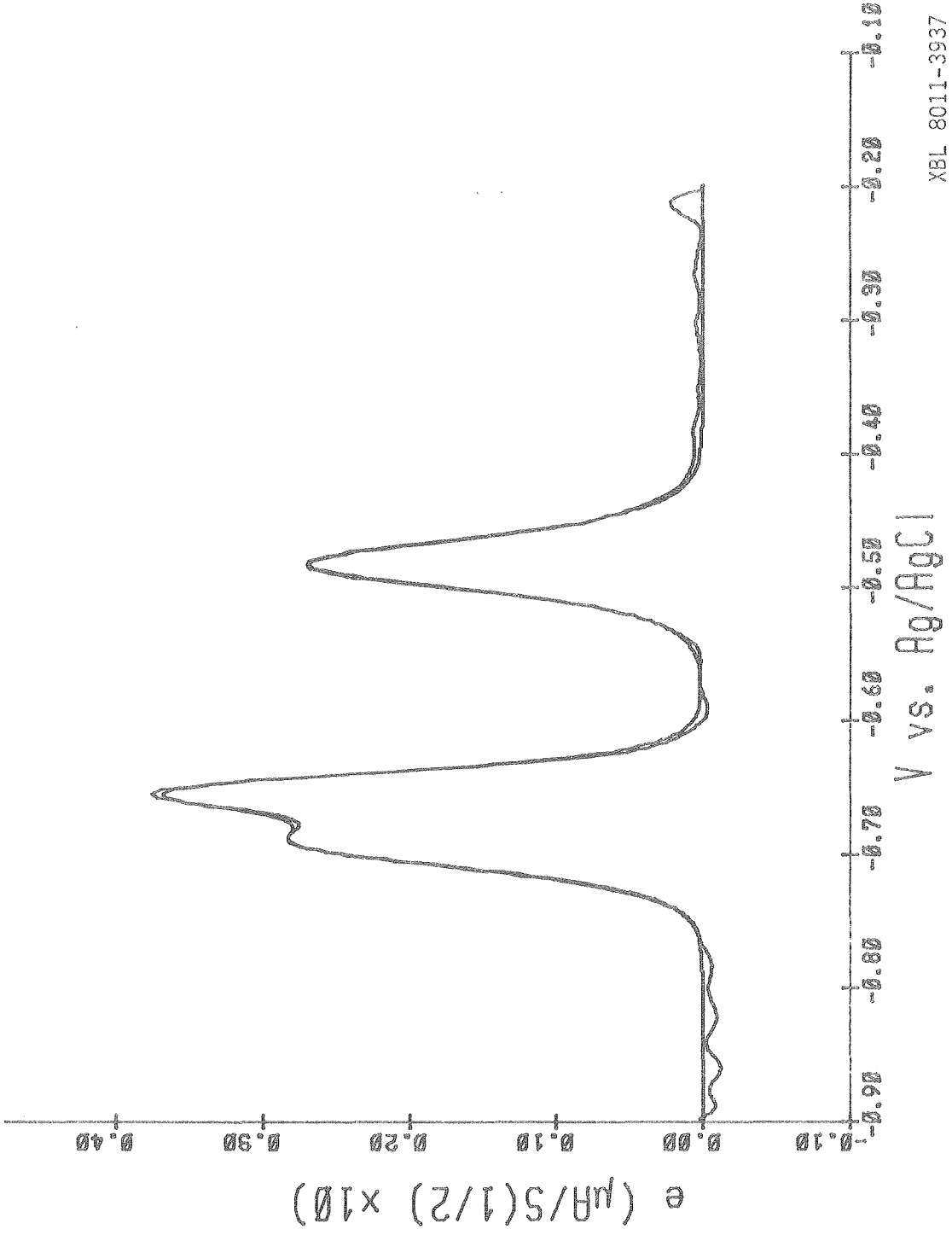
e (μA/S(1/2) x10)
0.40
0.30
0.20
0.10
0.00
-0.10
-0.90
-0.80
-0.70
-0.60
-0.50
-0.40
-0.30
-0.20
-0.10
V vs. Ag/AgCl
XBL 8011-3937

Figure 4

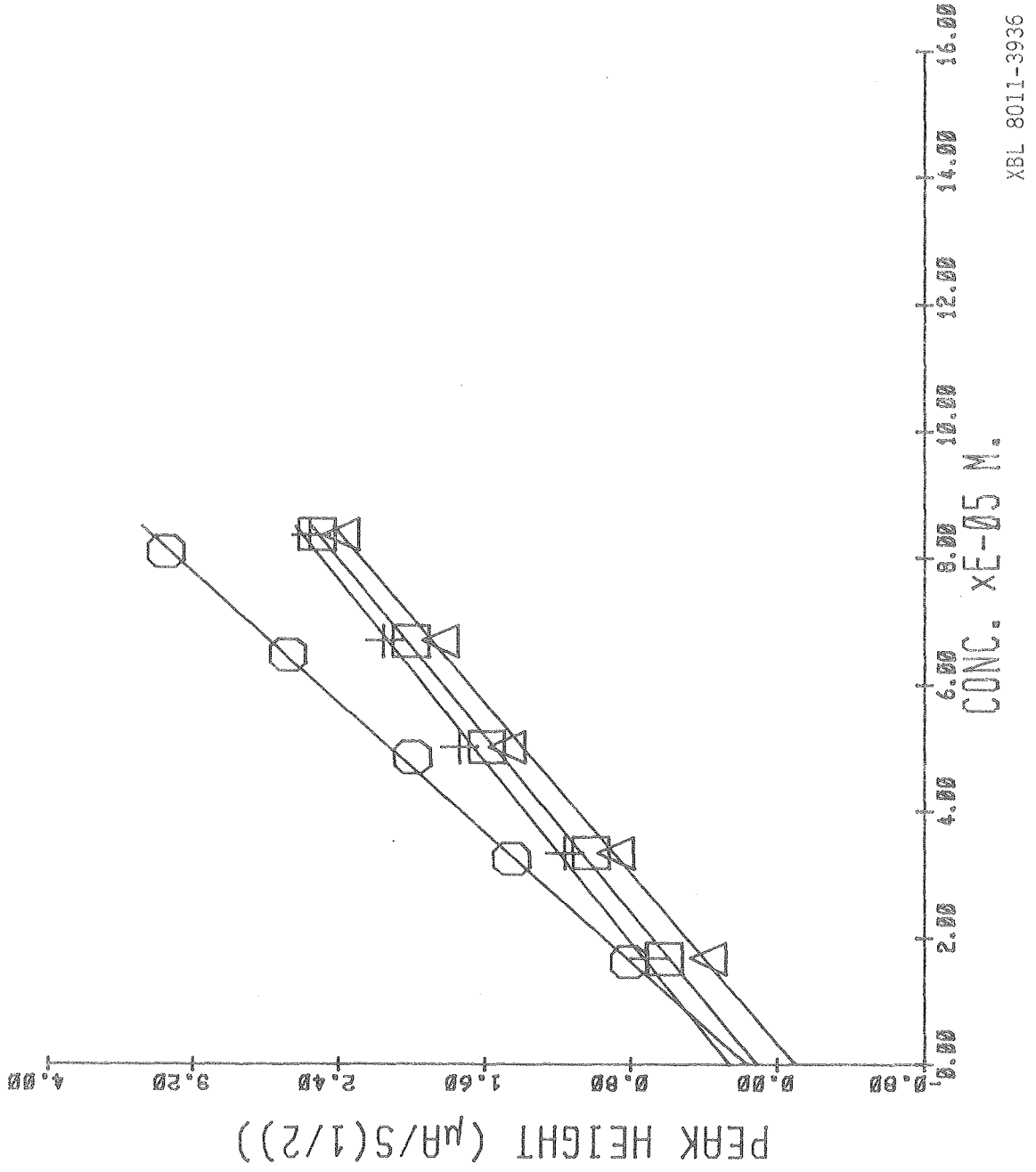
PEAK HEIGHT (μA/S(1/2))
0.00
0.80
1.60
2.40
3.20
4.00
0.00
2.00
4.00
6.00
8.00
10.00
12.00
14.00
16.00
CONC. xE-05 M.
XBL 8011-3936

Figure 5

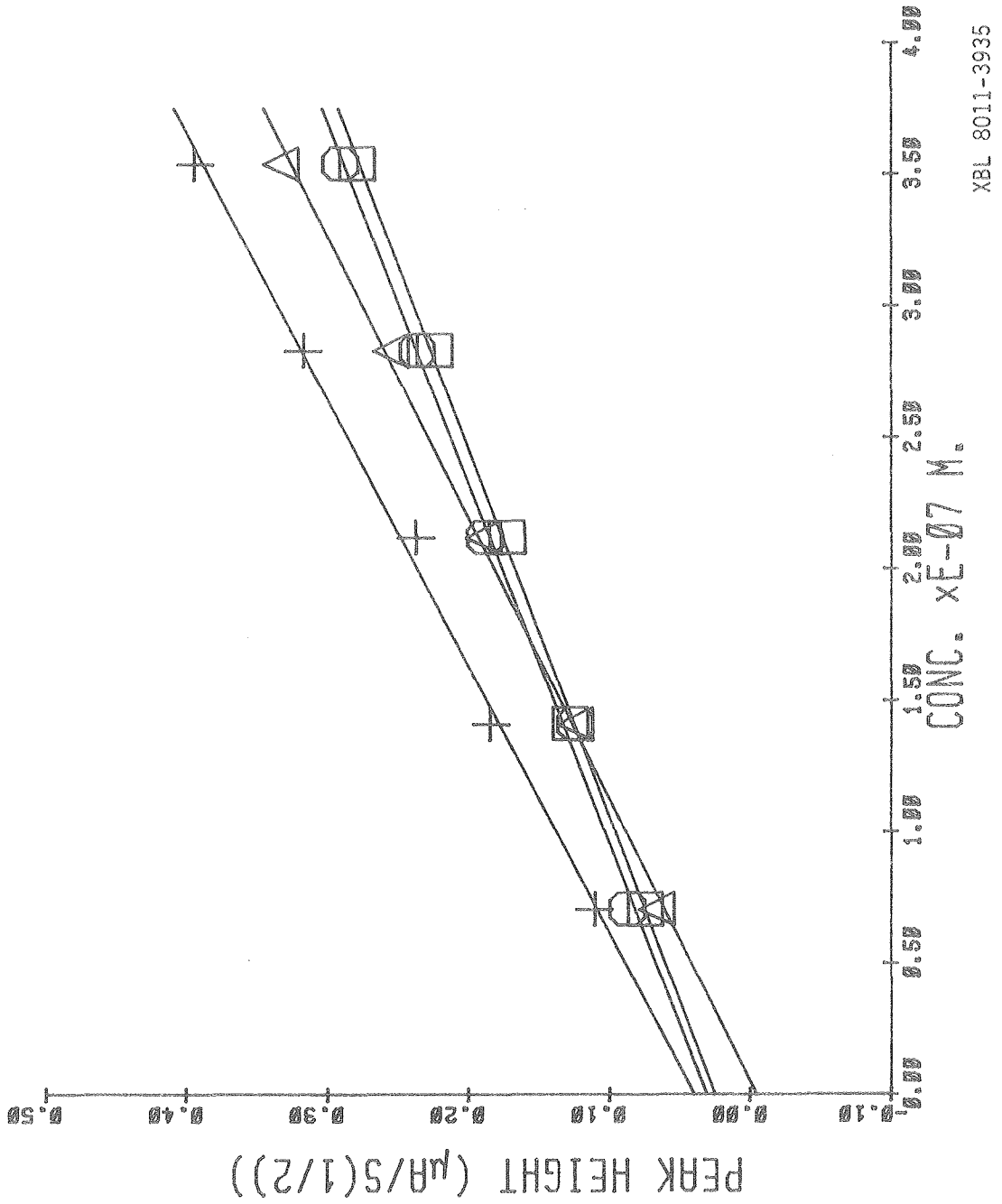
PEAK HEIGHT (μA/S(1/2))
0.00
0.10
0.20
0.30
0.40
0.50
0.50
1.00
1.50
2.00
2.50
3.00
3.50
4.00
CONC. xE-07 M.
XBL 8011-3935

Figure 6